Journal of Volcanology and Geothermal Research 73 (1996) 33–46

Journal of volcanology and geothermal research

Numerical modelling of stress generation and microfracturing of vesicle walls in glassy rocks

James E. Mungall *, Nicholas S. Bagdassarov, Claudia Romano, Donald B. Dingwell

Bayerisches Geoinstitut, Universität Bayreuth, D-95440 Bayreuth, Germany

Received 7 November 1995; accepted 4 March 1996

Abstract

In the absence of stress-concentrating flaws such as microfractures, vesicular glassy materials can withstand gas pressures within vesicles in excess of 100 MPa; however, vesicles within such materials are known to decrepitate explosively at much lower internal gas pressures, both in natural systems and in the laboratory. Here we present a model that quantitatively predicts the generation of microfractures in vesicle walls during cooling. Cooling of gas-bearing vesicles in glassy rock has little effect on water solubility in the glass, but leads to a rapid decrease in gas pressure in the vesicles. The drop in pressure causes disequilibrium between the water in the glass and in the vesicle. Dehydration of the glass in a diffusive boundary layer around the vesicle leads to elastic shrinkage. The resulting strain generates large tensile tangential stresses which can exceed the strength of the glass, causing microfracturing. Such microfractures present a possible means by which glassy rock surrounding vesicles could be weakened enough to permit explosive decrepitation at low pore vapor pressures. The results have implications wherever hydrous vesicular glasses are formed. For example rocks formed in shallow subvolcanic intrusions or vent plugs may spontaneously disintegrate with explosive emission of vapor; glassy submarine lavas spontaneously decrepitate upon dredging from the ocean floor (''popping rock''); vesicular glasses produced in laboratory experiments investigating vapor–melt phase equilibria have been observed to contain abundant fractures surrounding vesicles and to dehydrate at anomalously high rates.

Keywords: vesicle; overpressure; decrepitation; explosive; glass

1. Introduction

The behavior of vesicular glassy materials is of interest to many earth scientists, including volcanologists studying explosive silicic lava domes and shallow intrusions (e.g., Sato et al., 1992), geochemists analysing trace gases contained in vesicles of ocean floor basalts (e.g., Pineau and Javoy, 1994), and experimental petrologists investigating vapor–melt equilibria at high pressures (e.g., MacMillan, 1994; Romano et al., 1994a,b,1996). Whereas Romano et al. (1994a,1996) have shown that pristine, subspherical vesicles in glass can withstand internal overpressures on the order of 200 MPa without decrepitation, each of the works cited above contains descriptions of vesicular glassy materials whose vesicles were observed either to decrepitate violently or to drain

---

* Corresponding author. Fax: 049 921 553769. E-mail: james.mungall@uni-bayreuth.

0377-0273/96/$15.00 Published by Elsevier Science B.V.
PII S0377-0273(96)00017-0

away slowly through fractures at internal vapor pressures known or inferred to have been less than 5 MPa.

In this contribution we discuss the means by which relatively small internal gas pressures can generate stress concentrations sufficient to overcome the very high intrinsic strength of pristine glassy vesicle walls. We then propose a novel physical mechanism by which stress-concentrating microfractures can be generated in vesicle walls, and present the results of numerical modelling to support our idea. We conclude with examples of natural and experimental observations of low strengths of vesicular hydrous glasses which might be accounted for by our model.

1.1. Fracture mechanics of glass

The strength and fracture of glass can be satisfactorily described in the context of the fracture mechanics theory summarized in many recent works (e.g., Freiman, 1980; Pollard, 1987; Lawn, 1993). The theoretical breaking strength of cold glass is on the order of 10^{10} Pa; however, high temperature and submicroscopic defects can greatly reduce this value, by a factor of 10 to 100 (Freiman, 1980). Webb and Dingwell (1990) reported breaking strengths of $(1.0–5.0) \times 10^8$ Pa for rhyolitic and andesitic glass fibers at temperatures near to the glass transition temperature. The fibers had previously been annealed in the measuring apparatus, so that the glass–vapor interfaces in this case can be assumed to have been as smooth as the surface of a vesicle wall. Similarly, the tensile strengths of vesicle walls in feldspathic glasses are approximately 1.5×10^8 Pa in the temperature range 100–300°C (Romano et al., 1994a,1996); we assume therefore that fracturing of rhyolite glass will spontaneously occur whenever tensile stress exceeds 2×10^8 Pa.

The tangential component of stress in the wall of a spherical cavity is equal to 1.5 times the internal pressure, hence, decrepitation of spherical vesicles requires internal gas pressures on the order of 130 MPa. However, the stress exerted at the margin of a vesicle can be highly concentrated by favorable geometry. An elliptical hole in a two-dimensional sheet is a good conceptual model for a vesicle in a glassy medium. The stress at the point with the smallest radius of curvature varies according to the following relation after Inglis (1913):

$$\sigma_t = 2\sigma_x\left(\frac{c}{r}\right)^{\frac{1}{2}} \qquad (1)$$

where σ_t is the stress at the tip, the imposed stress (equivalent to pressure) is σ_x, in a cavity whose major axis measures $2c$ and whose smallest radius of curvature is r. Transfer of this simple model to three dimensional vesicles with irregular shapes is intractable analytically (cf. Tsuchida et al., 1982), but the principle can still serve as a useful guide (e.g., Lawn, 1993). Mungall (1995) pointed out that many intermediate to silicic dome lavas possess abundant vesicles whose shapes show a distribution of radii of curvature such that the radii of small embayments in vesicle walls might be up to 1000 times smaller than the radius of the vesicles themselves. In such cases, relatively small pore pressures would be expected to be able to cause spontaneous explosive decrepitation of the lava, leading to the generation of dangerous pyroclastic flows. Alidibirov and Dingwell (1995) have shown experimentally that this is the case, for internal vesicle gas pressure of 10 MPa in actual samples of dacitic lava from the cryptodome of Mt. St. Helens. In contrast, there exists a wide range of textures and vesicle gas pressures for which this mechanism cannot operate; any material whose vesicles do not have extremely convolute margins or whose internal gas pressure is far below 10 MPa will not be subjected to stress concentrations sufficient to cause fracture of the glass.

A further extension of Inglis' (1913) theory of notch stresses is to consider an ellipse whose smallest radius of curvature $r = 0$. In this case the cavity is a crack with a microscopically sharp tip, and Eq. (1) predicts a singularity in the stress field at the tip. In reality, the continuum model breaks down in the nearest neighborhood of the crack tip, a region called the process zone, where plastic deformation and parasitic fracturing come into play. The only barrier to the propagation of a crack is the energy required to form new surface within the crack, and to do the work involved in the process zone (Lawn, 1993).

The orientation of fractures depends on the stress deviator; a crack grows in a plane perpendicular to the least principal stress. If the sum of this stress and the internal vapor pressure in the crack is positive (tensile) then the fracture can grow, even if the external stress field in that direction is compressive (Pollard, 1987). Under large tensile stress a fracture can propagate at a speed approaching the elastic (sound) wave velocity in the glass, however, if it enters a region with a net compressive stress it will stop.

It is clear from the brief discussion above that the presence of even microscopic cracks in a glass surface will lead to a radical reduction of its effective strength. Any mechanism capable of generating such flaws in fresh glassy surfaces within vesicles will result in anomalously weak behavior of the surrounding glass in response to pressure imbalance between the vesicle and the ambient conditions.

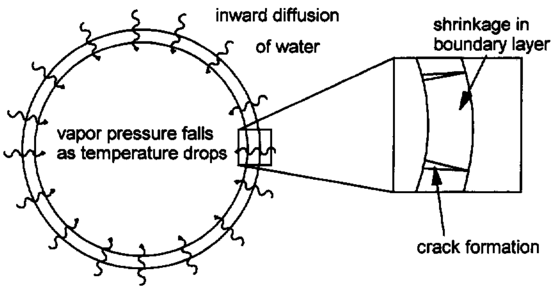

Fig. 1. Schematic illustration of a vesicle in the melt after cooling through T_g. The vesicle cannot shrink, so the vapor pressure decreases. Resultant dehydration of the vesicle walls creates a large tangential tensile stress. Microfractures form, penetrating to the depth of the diffusive boundary layer but cannot propagate farther because of compressive stress imparted on the outer part of the glass shell by the pressure difference between the vesicle and the external confining pressure.

2. Formulation of the problem

We will address cases in which hydrous glass is formed by cooling through the glass transition at pressures sufficient to retain an appreciable amount of water dissolved in the melt, and at which there is a free vapor phase consisting of pure water which can form vesicles. Crystallization is considered to be slow enough that a glassy mesostasis persists well below glass transition temperature. Thus vesicles remain isolated from one another within a glassy melt matrix unless connected by fractures. We use rhyolitic glass characteristics in our model; the unrelaxed mechanical properties of basaltic and intermediate glasses and melts differ very little from those of glasses of feldspathic or rhyolitic compositions (e.g., Manghnani et al., 1986; Kress et al., 1989; Webb and Dingwell, 1990; Kress and Carmichael, 1991).

Above the glass transition temperature (T_g) of the melt, vesicles respond to cooling by shrinkage accommodated by viscous relaxation of the surrounding melt. Below T_g, vesicle dimensions are frozen (Fig. 1) and the vapor in the vesicles is constrained to an isochore. This necessarily causes a drop in vapor pressure in the vesicle with further cooling. The solubility of water in the glass shows only a slight dependence on the diminishing temperature, increasing with decreasing temperature (Holtz et al., 1995), whereas the drop in vapor pressure consequent on lowering temperature causes the chemical potential of water in the vesicle to fall out of equilibrium with the chemical potential of water in the surrounding glass. The result is an inward diffusive flux of water from a boundary layer into the vesicle. Because the density of dry rhyolitic glass is higher than that of water-rich rhyolitic glass (e.g., Lange, 1994), the dehydration process will cause shrinkage of the glass in the diffusive boundary layer, thus generating tensile stresses tangential to the vesicle wall. If these tangential stresses exceed the tensile strength of the glass, radial cracks will form. If such a system is allowed to cool quiescently to ambient temperatures, a vesicular glass will be preserved. If, however, the confining pressure is released the residual vapor pressure in the vesicle will no longer be opposed by an external force, and the glass itself must then take up the stress applied by the pore vapor pressure. The existence of microfractures in the vesicle wall greatly lowers the bulk strength of the glass around the vesicle (Romano et al., 1994a,1996), and even very small drops in external pressures will be sufficient to extend the microfractures outward until they intersect each other. Thus the result of depressurization of the weakened glassy vesicular material may be sudden and spontaneous failure of vesicle walls leading to disaggregation of the bulk material, possibly on a very short (explosive) timescale.

Below we consider quantitatively the evolution of the stress field surrounding a vesicle within a portion of the glassy melt interior as cooling proceeds.

3. Assumptions

3.1. Geometry

We assume that the vesicular glass can be approximated as the sum of many close-packed spherical shells of glass, each with an impermeable outer wall and surrounding a water vapor-filled vesicle with which it is initially at chemical equilibrium. Use of a periodic boundary condition such as this is a common approximation in bubble growth studies (e.g., Arefmanesh and Advani, 1991) and allows implicitly for competition between bubbles for a finite amount of dissolved vapor. The assumption of an impermeable outer wall (zero flux condition) has the effect of simulating the presence of another identical bubble, reflected through the impermeable boundary. If the ratio between the vesicle radius and the outer shell radius is large enough, the modelled vesicle will sit in an essentially infinite reservoir, free of the interfering effects of other vesicles. By controlling this ratio we can simulate either isolated vesicles, or closely spaced ones with strong competition for dissolved water.

In cases of very large vesicles, rapid cooling, or very slow diffusion of water, the process will be confined to a very narrow boundary layer in the glass adjacent to the vesicle, and the geometry could be reduced to a half-space—this approach may be useful for quick estimates of the likelihood of formation of fractures.

3.2. Mass transport

We have treated transport of water in the glass following the approach of Zhang et al. (1991), with a diffusion coefficient that is a very strong function of water content. Although the speciation model used by Zhang et al. (1991) has been shown to be inaccurate in detail (Nowak and Behrens, 1995; Shen and Keppler, 1995), their diffusion model as a whole succeeds well at duplicating observed water diffusion profiles in glass for the range of water contents of interest here (i.e., less than 2 wt.%), because it was calibrated against experimental data in that range.

The diffusion of water is complicated by the fact that water exists in glasses and melts as both hydroxyl groups (OH) and molecular water (H_2O), related by the speciation reaction:

$$H_2O + O_m = 2\,OH \qquad (2)$$

where O_m refers to any unprotonated oxygen ion in the melt structure. An equilibrium constant K can be defined as:

$$K = \frac{[OH]^2}{[H_2O][O]} \qquad (3)$$

where [O] is taken to be the mole fraction of all unprotonated oxygen in the melt (Stolper, 1982). Although there has been considerable debate about the temperature, composition, and quench-rate dependance of the apparent value of K as it is measured in glasses (e.g., Webb and Dingwell, 1990; Zhang et al., 1991; Nowak and Behrens, 1995; Romano et al., 1995; Shen and Keppler, 1995; Zhang et al., 1995), to a first approximation it may be modelled as being broadly independent of composition and water content, greatly simplifying the ensuing calculations at the cost of an uncertainty in K of less than 0.1 log unit. We have fit the data of Zhang et al. (1991) (Fig. 6) and Zhang et al. (1995) (Fig. 5) with the following empirical expression:

$$\ln k = -\frac{2900}{T} + 1.28 \qquad (4)$$

where T is the absolute temperature.

The diffusive flux of water in glass depends on the sum of the fluxes of H_2O and OH, as is shown by the following adaptation of the diffusion equation (after Wasserburg, 1988):

$$\frac{\partial c_W}{\partial t} = \frac{1}{r^2}\frac{\partial}{\partial r}\left(D_{H_2O} r^2 \frac{\partial C_{H_2O}}{\partial r} + D_{OH} r^2 \frac{\partial C_{OH}}{\partial r}\right) \qquad (5)$$

where c_W is the bulk water concentration in the glass, c_{OH} is the concentration of OH and c_{H_2O} is the concentration of molecular water, r is the distance from the origin, and D_{OH} is the diffusion coefficient of hydroxyl groups and D_{H_2O} is the diffusion coefficient of molecular water. We use radial coordinates for simplicity and accuracy; similar solutions can be developed for infinite planar configurations, but are less applicable to the geometry of curved vesicle surfaces.

The diffusivity of OH has been shown to be negligible at water contents in the concentration range of interest whereas diffusion coefficients D_{H_2O} ($m^2\ s^{-1}$) for molecular water in rhyolite glass may be given by the following Arrhenius relationship (Zhang et al., 1991):

$$\ln D = -14.59 - \frac{1.03 \times 10^5}{RT} \qquad (6)$$

where R is the ideal gas constant (8.314 $J\,K^{-1}\,mol^{-1}$) and T is temperature in kelvins, if these diffusion coefficients are used in conjunction with the solution model for water speciation used by Zhang et al. (1991).

3.3. Equations of state

Pressure in the vesicle can be related to the water concentration in the vesicle wall, assuming chemical equilibrium between water activity in the vapor and glass at the interface; for this we use the following Henry's law relationship (Wilson and Head, 1981):

$$c_w = 0.0013 P^{\frac{1}{2}} \qquad (7)$$

where P is the vesicle vapor pressure in bars and c_W is the weight fraction of water in the glass. This equation is in agreement with data for rhyolitic and feldspathic melts (Silver et al., 1990; MacMillan, 1994; Behrens, 1995) and is based on the assumption that water dissolves in the glass exclusively as OH according to Eq. (1), and that ideal mixing occurs among the three oxygen-bearing species described in Eq. (2)). This equation deviates from reality to the extent that molecular water is able to dissolve in the glass; however, it is clear from numerous studies (e.g., Silver et al., 1990; Nowak and Behrens, 1995) that the overwhelming majority of water present at low water contents is indeed present as OH groups. Any departure of Eq. (7) from the true solution behavior will overestimate the solubility of water in the glass, with the result that we may slightly underestimate the rate at which water concentration in the vesicle wall drops during cooling.

Water pressure in the vesicle is assumed to conform to a Redlich–Kwong type equation of state (Halbach and Chatterjee, 1982), and for simplicity we assume that water is the only volatile species present.

Dilatation of the glass due to changing water content is described by a simple linear coefficient of expansion:

$$\alpha = \frac{1}{\rho^0} \frac{\partial \rho}{\partial C_w} \qquad (8)$$

where ρ is the glass density and ρ^0 is the density of the dry glass; we have adopted a value for alpha of -1.0 (cf. Shaw, 1974; Silver et al., 1990; Lange, 1994; Romano et al., 1994b). We have calculated Young's modulus $E = 5.08 \times 10^{10}$ Pa and Poisson's ratio $\nu = 0.18$ from the data of Bagdassarov et al. (1993). Data for the several compositions studied by Bagdassarov et al. (1993) show that the dependence of shear modulus on temperature is on the order of 10% over the temperature range from 20 to 670°C, a negligible effect. Similarly, the variation of bulk modulus with temperature over this range can be estimated to be less than 25% (cf. Mazurin et al., 1983; Webb, 1991).

3.4. Stress field

Stress depends on the displacement induced by the pressure differential between the vesicle and the far-field, and by dilatation resulting from changes in water content. A general solution to the problem of thermal stress in a hollow sphere is given by Nowacki (1986, p. 219). The thermal stress problem is exactly analogous to a compositional gradient stress problem (Ernsberger, 1980; Mungall, 1994). We set boundary conditions for the gradient stress problem such that normal stresses on the inner and outer boundaries of the shell are zero. We then add to the solution of this problem the stresses resulting from the pressure differential between the vesicle and the far-field pressure, taken to be equal to the confining pressure at zero time. The stress distribution in the hollow sphere for these boundary conditions is as follows:

$$\sigma_{rr} = \left\{ \Delta P \left[1 - \left(\frac{a}{r} \right)^3 \right] \Big/ \left[\left(\frac{a}{b} \right)^3 - 1 \right] \right\} - \frac{2E\alpha}{(1-\nu)(a^3-b^3)} \left[\left(\frac{a}{r} \right)^3 \int_b^r c\rho^2 \, d\rho + \left(\frac{b}{r} \right)^3 \int_r^a c\rho^2 \, d\rho - \int_b^a c\rho^2 \, d\rho \right] \tag{9}$$

$$\sigma_{\phi\phi} = \sigma_{\theta\theta} = \left\{ \Delta P \left[1 + \frac{1}{2} \left(\frac{a}{r} \right)^3 \right] \Big/ \left[\left(\frac{a}{b} \right)^3 - 1 \right] \right\} + \frac{E\alpha}{(1-\nu)(a^3-b^3)} \left[\left(\frac{a}{r} \right)^3 \int_b^r c\rho^2 \, d\rho + \left(\frac{b}{r} \right)^3 \int_r^a c\rho^2 \, d\rho + 2\int_b^a c\rho^2 \, d\rho - c(a^3-b^3) \right] \tag{10}$$

where a is the outer radius of the spherical shell, b is the vesicle radius, E is Young's modulus of the glass, ν is Poisson's ratio of the glass, $C = c_{W_0} - c_W$, c_W is water concentration at radius r and time t, and c_{W_0} is the initial water concentration of the glass. The subscripts rr, $\phi\phi$, and $\theta\theta$, respectively, identify the radial and two tangential directions in the coordinate space. ΔP is the difference between the confining pressure on the system and the vapor pressure in the vesicle. When two vesicles are close together the stress fields created by their local water concentration gradients will overlap; however, as the ensuing analysis shows, the large magnitude stresses that concern us are extremely localized in the diffusive boundary layers surrounding vesicles, so that we can effectively neglect vesicle–vesicle interactions of the stress field.

To a first approximation, which is exact in the case of extremely slow water diffusion or isolated vesicles, the stress depends solely on the change in concentration between the vesicle wall and the bulk glass. For the chosen elastic parameters, Eq. (10) allows us to calculate that a change in water concentration of 0.32 wt.% will generate 200 MPa of tensile tangential stress in the wall of an isolated vesicle, sufficient to fracture the vesicle wall.

4. Numerical model

We have modelled the evolution of stress surrounding a vesicle in a cooling vesicular glass. Stresses depend on the change in water concentration in the glass and upon the pressure exerted on the glass by the vapor in the vesicle. The calculation therefore hinges on the evolution in time of the water concentration profile in the glass. An analytical solution to Eqs. (2)–(7) could not be found, due to the complex time-dependence of both the diffusion coefficient of water, and the vesicle vapor pressure, which in turn affects the concentration of water in the vesicle wall, a boundary condition for the diffusion equation. This difficulty cannot be overcome by resorting to a simplified model geometry; instead, we used an explicit finite difference form of Eq. (5) to model the diffusion of water (Crank, 1975, p. 144; Zhang et al., 1991). To ensure stability of the resulting solutions we set the parameter $D_{H_2O}\delta t/\delta r^2$ to be equal to 0.4 at each timestep, by adjusting the duration of the timestep. At each timestep in the calculation the temperature is updated to reflect cooling of the system at a given cooling rate. The concentration profile from the previous timestep is integrated numerically to find the amount of water that has diffused into the vesicle; this quantity is added to the initial water content of the vesicle and used to find a new vapor pressure from the equation of state. The separate concentration profiles of OH and H_2O are calculated from the bulk water concentration profile using Eq. (3) and Eq. (4). The diffusion coefficient D_{H_2O} is recalculated according to Eq. (6), a new concentration and speciation of water at the vesicle wall is calculated from the new vapor pressure using Eq. (7), and these two quantities are combined with the zero flux condition at the outer wall of the glass shell to calculate a new concentration profile for molecular water. Addition of this profile to the (unchanged) OH concentration profile gives a new bulk water concentration profile to be used as input to the next timestep. Recall that the zero flux condition implicitly models the existence of another vesicle an equal distance away, so that the diffusion profile can be considered to be reflected through the outer boundary of the glass shell under consideration. When the temperature reaches the ambient temperature (300 K), corresponding to complete cooling (and complete depressurization of the vesicle), or when the stress in the vesicle wall exceeds 2.0×10^8 Pa, corresponding to initiation of microfracturing in the vesicle wall, the simulation is stopped. Continuation of the modelling to temperatures below 400°C requires extrapolation of the diffusion model of Zhang et al. (1991) outside the range of temperatures at which it was calibrated. We feel justified in doing so because Zhang et al. (1991) were able to extrapolate their results, based on low-temperature experiments on glasses, to match the data of earlier workers based on experiments in melts at very much higher temperatures (Karsten et al., 1982; Lapham et al., 1984). The success of the diffusion model in extrapolating across a wide range of temperatures including T_g suggests that extrapolation over smaller temperature ranges without a change in physical state should be safe.

We have run the model to approximate conditions likely to arise both in cooling magmas and in quenched experimental runs. Adjustable input parameters are: (a) initial water content of glass; (b) glass transition temperature (i.e., temperature at which the simulation begins); (c) vesicle size and spacing; and (d) cooling rate.

4.1. Water content of the glass

We have restricted our modelling to the range of water contents over which we have actual measurements of viscosity of the melt, and over which the diffusion model of Zhang et al. (1991) was calibrated. Our highest modelled water content of 1.85 wt.% corresponds to a confining pressure at T_g of 20.25 MPa; our lowest modelled water content of 0.41 wt.% corresponds to a confining pressure at T_g of only 2.13 MPa. These values all fall within the range of water contents measured in obsidian from near-surface environments (Melson, 1983; Taylor et al., 1983; Newman et al., 1986, 1988; Blank et al., 1994).

4.2. Glass transition temperature

The glass transition temperature controls the temperature at which the vesicle dimensions become frozen, and at which their internal pressures begin to drop out of equilibrium with the water dissolved in the surrounding glass.

T_g is strongly dependent on water content; for rhyolitic glasses near to haplogranitic compositions it is a relatively weak function of variations in other chemical components. To allow explicitly for compositional variation we have employed experimental temperature–viscosity relations for melts with water contents between 1.85 and 0.41 wt.% (Dingwell et al., 1996). Where experimental data were lacking we interpolated on a plot of T_g versus total water content. In doing so we neglect that fact that T_g also depends upon cooling rate, varying by as much as 30°C per decade in cooling rate (Stevenson et al., 1995). The effect of this reduction of T_g with decreased cooling rate will be to compress the phase of diffusive re-equilibration between glass and vapor into a shorter time interval, however, it will not affect the magnitudes of the stresses calculated, because we have assumed that the solubility of water in the glass depends only on the confining pressure (which does not depend on T_g).

4.3. Cooling rate

In the interior of even a small magma body heat loss is conductive and relatively slow; in contrast, the propagation of an advectively cooled hydrothermal regime down into the conductively cooled magmatic regime (Hardee, 1980; Dzurisin et al., 1990) results in comparatively rapid quenching from near-magmatic temperatures to 100°C at the hydrothermal front. The final cooling rate of an individual portion of a vent plug or cryptodome is thus likely to be dictated by distance from one of a developing system of joints with meter-scale spacings. Cooling rates can therefore be assumed to be well approximated by a conductive cooling model with a maximum distance from the cool boundary on the order of one to ten meters. To avoid a confusing proliferation of model cooling histories we have chosen to use constant cooling rates of 10^1 and 10^2 $\mathrm{K\,s^{-1}}$ to correspond to experimental quench rates, and 10^{-1}, 10^{-2}, 10^{-3}, 10^{-4} and 10^{-5} $\mathrm{K\,s^{-1}}$ to correspond to natural cooling rates at which glass might be expected to be preserved. The latter corresponds to a cooling period of several months to cool to ambient temperature near 100°C. The slowest rate we have chosen corresponds to a distance of about 1 m between the joint and the vesicle, assuming thermal diffusivity of 10^{-2} $cm^2 s^{-1}$ (e.g., Spera, 1980; Snyder et al., 1994). On the length-scale of a single vesicle, temperature has no spatial gradient because the diffusion coefficient for heat transfer is several orders of magnitude greater than that for water diffusion even at the highest temperatures treated in our model. Our results will only apply to relatively small and shallow intrusive bodies or plugs, or to crusts forming on submarine lava flows, where the overlying water column applies a confining pressure. In very large (hundreds of meters) intrusions, the early slow cooling will last long enough to dominate the cooling history of the rock, permitting both devitrification and the erasure of gradients in water concentration.

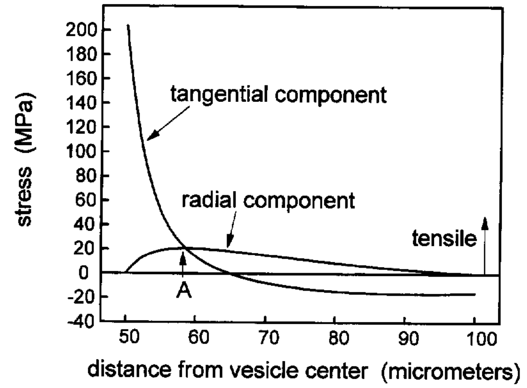

Fig. 3. Distribution of stress around the vesicle of Fig. 2, at the time of microfracture initiation. The very large tensile tangential stress falls off rapidly with increasing distance from the vesicle, becoming equal in sign and magnitude (isotropic stress field) at a distance of about 10 μm from the vesicle wall, at the radius marked *A*. The radial stress component is everywhere tensile.

5. Results and discussion

We first present in detail the results of a single representative simulation, to illustrate the important features of the stress field produced during cooling of the vesicle and glass. In this simulation the initial water content is 1.33 wt.%, giving an initial vesicle pressure of 10.46 MPa. The cooling rate is 10^{-4} $K s^{-1}$; cooling from T_g at 774–533 K takes about 30 days. The model vesicles are 100 μm in diameter and spaced on 200 μm centers. Fig. 2 shows the concentration of water at intervals of 5.0×10^5 s from the time at which the melt passes through the glass transition until the tangential stress in the vesicle wall exceeds 2×10^8 Pa and the run is terminated. For the first two weeks, as the temperature drops some 150 K, the rate of diffusive re-equilibration of water in the glass with vapor pressure in the vesicle is such that the concentration profile remains approximately flat. The overall concentration in the glass thus drops from 1.33 to about 1.25%. Since the stress in the vesicle wall depends on the difference between the wall concentration and the far-field concentration, there is negligible stress generated during this initial phase of cooling. With further cooling, the diffusion coefficient of water decreases so much that the glass farthest from vesicles is effectively prohibited from re-equilibrating with the decreasing pressure in the vesicles, and the concentration gradient steepens until the difference between the wall concentration and the far-field concentration exceeds the critical value of approximately 0.32% that we discussed in the formulation of the problem.

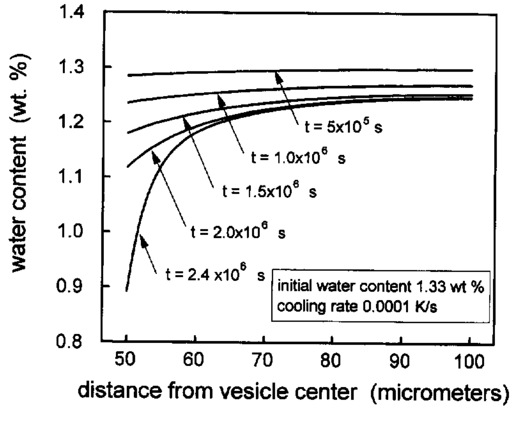

Fig. 2. Water concentration in glass shell with 100 μm radius surrounding 50 μm vesicle. Cooling rate 10^{-4} $K s^{-1}$, initial water content 1.33%. Each profile represents the distribution of water at the indicated time in seconds. During the first 1.5×10^6 s the water concentration decreases smoothly throughout the glass volume. Continued cooling depresses the diffusion coefficient and permits the establishment of a large concentration gradient.

The resulting stress field at the time of fracture (tangential stress exceeds 2.0×10^8 Pa) is shown in Fig. 3. The magnitude of the tensile stress drops away radially until at a distance of less than 10 μm from the vesicle wall it is equal in sign and magnitude to the radial stress component. The radial stress component is everywhere positive, except at the vesicle wall and outer boundary, where it is zero. In a stress field such as this, any fracture would be initiated in the vesicle wall, and would not be expected to penetrate beyond the region of large tensile stresses. We therefore expect that, when the tangential stress exceeds the strength of the glass, a number of radial cracks will form and penetrate approximately 10 μm before stopping. As long as the external pressure on the glass is subequal to the internal vapor pressure the fractures will not propagate any farther. In the presence of moderate tensile radial stress, the fracture might be expected to inflect near the point at which the tangential and radial stress components are equal, and subsequently propagate in a surface oriented as a concentric shell surrounding the vesicle at the distance of maximum radial stress component, as has been observed in experimental analogues (Romano et al., 1996).

Fig. 4 shows the pressure–temperature paths followed by the contents of vesicles initially in equilibrium with glasses containing water contents ranging from 1.85 to 0.41%, all with the same geometry as in the example above, but with a faster cooling rate of 10^{-1} $\mathrm{K s^{-1}}$ to facilitate running of the numerical model. Each curve starts from the right, at the temperature of the glass transition and the pressure both determined by the water content. The first segment of each curve is essentially an isochore in the phase diagram of water, deflected upward slightly due to the gradual increase in water content (density) of the inclusion. As each curve intersects the two-phase curve for water, it is constrained to follow it down with a much greater P–T slope than it initially had. Each curve ends where the calculated tensile stress in the vesicle wall exceeded the breaking strength of the glass. It is clear from Fig. 4 that glasses starting with higher water contents are able to form microfractures at higher temperatures and vapor pressures; any glass with less than about 0.4% of water at T_g should not form any fractures at all.

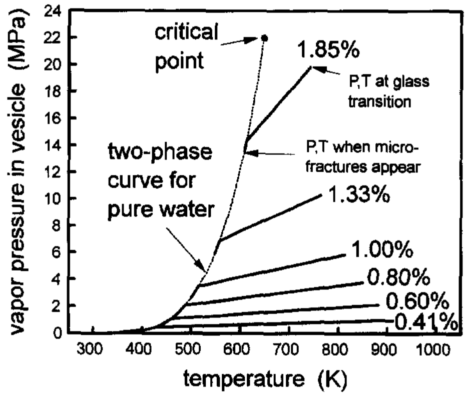

Fig. 4. Pressure versus temperature for vapor in vesicle. Each curve represents the path followed by contents of one vesicle surrounded by glass starting with the indicated water content. Each curve terminates at the conditions at which microfractures form. Sharp inflections appear where P–T paths intersect the liquid–vapor curve.

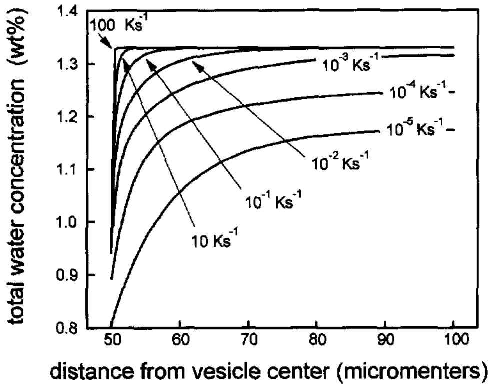

Fig. 5. Concentration profiles at time of microfracture initiation for a range of cooling rates for 50 μm vesicle radius and 50 μm shell thickness, and initial water content of 1.33%. The width of the diffusive boundary layer increases with decreasing cooling rate.

We varied the cooling rate and the vesicle size to test the importance of these parameters. Fig. 5 shows the concentration profile at the time when wall stress exceeded the strength of the glass for 50 μm radius inclusions cooled at rates ranging from 10^2 to 10^{-5} $\mathrm{K s^{-1}}$, with initial water content of 1.33%. The effect of faster cooling is to narrow the diffusive boundary layer, thus allowing stress to build up faster than in the slower cooling case. This effect also causes deflection of P–T paths to higher pressures with decreasing cooling rate (not shown). Varying the external radius from 200 to 60 μm while keeping the vesicle radius at 50 μm has an analogous effect (Fig. 6). Vesicles with wide mar-

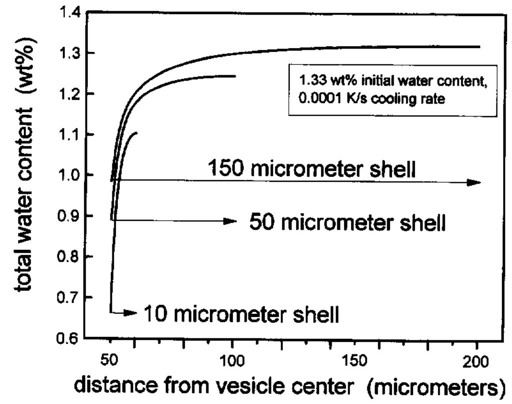

Fig. 6. Concentration profiles at time of microfracture initiation for a range of vesicle shell widths, all with a 50 μm vesicle radius. Competition for water between closely spaced vesicles (thin shells) delays formation of large concentration differences, inhibiting microfracturing.

gins are effectively isolated in infinite reservoirs, and their internal pressures are buffered by the water content of the surrounding glass until the diffusion coefficient has fallen considerably. Vesicles with thin walls interact extensively, effectively drawing water out of the walls and thus suppressing the development of large concentration gradients and stresses until the temperature (and temperature-controlled diffusivity of water) is very low. Widely separated vesicles are therefore the first to generate microfractures.

6. Application of the model

6.1. Natural examples

The application of this model to shallow intrusions or lava flows depends on the accuracy and appropriateness of the parameters we have chosen. Our aim at this point is not to construct a detailed model of a partaicular cooling magma body or volcanic facies and predict where and when explosive failure will occur. Rather, we wish to show that vesicular, water-bearing glasses should be expected to develop microfractures in their vesicle walls during cooling, strictly as a result of diffusive exchange of water between the glass and vesicles. As has been documented by Romano et al. (1994a,b,1996), the appearance of microfractures has dramatic effects on the confining strength of glass around vesicles, and can account very well for the common observation that cooled, glassy rock surrounding vesicles has tensile strength approximately equal to the internal vapor pressure of a few bars.

The critical parameter on which the model rests is the initial water content of the glass, which, for a continuously degassing magma, depends primarily on the confining pressure exerted on the local environment. At the slow effusion rates typical of dome-forming eruptions the water content can be taken to be approximately in equilibrium with the magma hydrostatic pressure as excess degassed water escapes from the ascending magma column in the vent (e.g., Eichelberger et al., 1986; Woods and Koyaguchi, 1994). The assumption of equilibrium between water content and magma pressure is supported by the fact that the incubation time of new vesicles in depressurized magma is on the order of seconds (Hurwitz and Navon, 1994), so that at slow flow rates, any underpressure of more than 1 MPa will be immediately compensated for by the growth of new vesicles in previously bubble-free domains. Consequently, the water content at the time of cooling through T_g can be derived directly through Eq. (7) from the estimated intrusion pressure. The confining pressure is likely to be considerably less than the tensile strength of the enclosing rock due to the presence of fractures. Assuming instead that the pressure is a passively exerted lithostatic pressure, we can estimate the range of depths of burial at which the proposed mechanism might operate. A pressure of 7.5 MPa would be exerted in a shallow intrusion under 300 m of material with a bulk density of 2500 $\mathrm{kg\,m^{-3}}$. Self et al. (1979) estimated carapace strengths of 10–20 MPa; this range of pressures corresponds to water contents of 1.3–1.84 wt.%. If we allow for the relatively conservative possibility that the tensile strength of either the enclosing rock or of the quenched margin of the shallow intrusion is of the order of 5 MPa then we find that *any* shallow intrusion that had not previously equilibrated to atmospheric pressure could cool through the glass transition temperature with water contents in the glass as high as 0.9 wt.%.

Extension of the model to subaerial extrusive bodies such as exogenous domes or lava flows is questionable, since such materials are as a rule not observed to contain more than about 0.5% dissolved water. However, at active endogenous dome complexes, the distinction between a shallow intrusion and a dome growth event is blurred, particularly if spines of solid lava solidify at shallow depths but are then extruded above the dome surfaces (e.g., Mt. Pélée in 1902 and 1903; Jaupart and Allègre, 1991).

Finally, it is important to note that lavas have access to more than one mechanism for explosive disaggregation—the mechanism we have proposed can work in concert with the stress-concentrating effects of irregular vesicle shapes. For example, consider a 2000 μm vesicle in a glass with an initial water content of 0.6 wt.%. Cooling of this vesicle from T_g at 885–655 K causes internal pressure to fall from its initial value of 2.13–1.6 MPa. Consequent diffusion of water into the vesicle leads to the generation of a tensile tangential stress around its margins of 50 MPa, an amount insufficient to cause brittle failure of the glass. However, if this vesicle has an irregular shape, with small embayments on the order of 0.5 μm in radius, then a release of the confining pressure on the glass would lead to the imposition of a concentrated stress at the tips of the embayments on the order of 150 MPa. Superposition of the stresses resulting from dehydration and stress concentration produces localized stresses of 200 MPa, sufficient to fracture the glass, despite the fact that neither stress-concentrating mechanism could work alone to produce this result.

A further example of a natural system in which spontaneous decrepitation of vesicles occurs at low internal pressures is ''popping rock'' dredged from the ocean floor. The material in this case is vesicular basaltic glass with sub-spherical vesicles and total water content on the order of 0.5 wt.% (Pineau and Javoy, 1994). Although the presence of CO_2 complicates the pressure–temperature relationships in the gases trapped within the vesicle, inspection of the phase diagram of $CO_2 + H_2O$ (e.g., Roedder, 1984, p. 229) shows that the pressure of the gas mixture would be near to 1 MPa at 10°C, the approximate temperature of deep ocean water. It is clear, therefore, that the equilibrium water concentration in the vesicle walls will fall to nearly zero during cooling, with the result that a change in water concentration of more than 0.32 wt.% is expected to develop during quench of the glass. In this case, microfractures are expected to develop in the margins of the vesicles. Dredging of microfractured vesicular basaltic glass removes the confining pressure exerted by the seawater column; samples initially at temperatures less than 10°C would remain stable on the ship's deck. Warming of the sample in air to temperatures near 25°C will raise the internal pressure to several MPa, resulting in spontaneous decrepitation of vesicles (''popping'') during the minutes or hours following sample collection.

6.2. Experimental examples

There are several examples in the literature in which synthetic vesicular glasses have been found to show anomalous loss of water on timescales of days or weeks (Paillat et al., 1992; MacMillan, 1994; Romano et al., 1994a,b,1996). The rate of water loss in some of these examples greatly exceeds the flux possible by bulk diffusion through the glass, and requires that transport has occurred through fractures, to drain vesicles (Romano et al., 1996). Our modelling results show that water-rich vesicular glasses should *always* develop microfractures during quench, no matter how fast the quench rate. Romano et al. (1996) apply our microfracturing model to their observations, and provide evidence for the presence of microfractures, in the form of TEM micrographs of radial fractures.

7. Conclusions

There is a discrepancy between known, very high strengths of glass surrounding vesicles and the observed weak response of some vesicular glassy rock to its own vesicle overpressure both in nature and in experimental studies. This discrepancy may be accounted for by considering the stresses that must appear as the system is cooled and water attempts to find a new equilibrium between vesicle pressure and its concentration in the glass. Cooling forces water vapor pressure in vesicles to fall, driving diffusion of water from the glass into the vesicle. The dehydrated boundary layer in the vesicle wall shrinks and is subjected to tensile tangential stresses sufficient to induce radial microfracturing under a very wide range of cooling rates and vesicle geometries. The first order control on fracturing behavior is the initial water content of the glass. Melts which pass through their glass transition temperature with water contents between 1.85 and 0.4%, corresponding to confining pressures between approximately 20 and 1 MPa, are expected to develop microfractures in their vesicle walls. The microfractures will initially propagate only a few microns before being arrested by a far-field compressive stress. These fractures may respond to unloading of the vesicle-glass system by catastrophic propagation and intersection, to cause complete disaggregation of the formerly solid rock. Typical lava with initial water content below 0.6% is unlikely to show this type of behavior, however, the combined effects of stresses generated by dehydration and stress concentration in irregularly shaped vesicles may cause anomalously weak behaviour of glassy lava at the lower water contents $< 0.6\%$ observed in the field.

Observations of spontaneous decrepitation of vesicles in basaltic glass dredged from the ocean floor are also accounted for qualitatively by the dehydration–microfracturing model, although we have not run the numerical model quantitatively due to the complicating effects of CO_2 on the vapor phase relations.

Experimental observations of very low strength of water-bearing vesicles and long-term leakage of water from vesicles are also accounted for by the development of microfractures during quench and dehydration of the diffusive boundary layer surrounding the vesicles.

Acknowledgements

This work has benefited from discussions with F. Busse, P. MacMillan, M. Nowak, R. Stevenson and S. Webb, and from reviews by Curtis Manley and two anonymous reviewers. J. Mungall was supported by an Natural Sciences and Engineering Research Council of Canada postdoctoral fellowship and by the Bayerisches Geoinstitut Visitor's Program while this work was being done.

References

Alidibirov, M. and Dingwell, D.B., 1995. Experimental study of highly viscous magma fragmentation in explosive volcanic eruptions. Per. Mineral., 64: 71–72.

Arefmanesh, A. and Advani, S.G., 1991. Diffusion-induced growth of a gas bubble in a viscoelastic fluid. Rheol. Acta, 30: 274–283.

Bagdassarov, N.S., Dingwell, D.B. and Webb, S.L., 1993. Effect of boron, phosphorus and fluorine on shear stress relaxation in haplogranitic melts. Eur. J. Mineral., 5: 409–425.

Behrens, H., 1995. Determination of water solubilities in high-viscosity melts: An experimental study on $NaAlSi_3O_8$ melts. Eur. J. Mineral., 7: 905–920.

Blank, J.G. Gardner, J.E. and Jaupart, C., 1994. Degassing and fragmentation histories of erupted magmas: evidence from matrix glasses in pumice. Eos, 75: 719.

Crank, J., 1975. The Mathematics of Diffusion. Oxford Univ. Press, Oxford, 2nd ed.

Dingwell, D.B., Romano, C. and Hess, K.-U., 1996. The effect of water on the viscosity of a haplogranitic melt under $P-T-X$ conditions relevant to silicic volcanism. Contrib. Mineral. Petrol., 124: 19–28.

Dzurisin, D., Denlinger, R.P. and Rosenbaum, J.G., 1990. Cooling rate and thermal structure determined from progressive magnetization of the dacite dome at Mount St. Helens. Washington. J. Geophys. Res., 95: 2763–2780.

Eichelberger, J.C., Carrigan, C.R., Westrich, H.R. and Price, R.H., 1986. Non-explosive silicic volcanism. Nature, 323: 598–602.

Ernsberger, F.M., 1980. Techniques of glass. In: Elasticity and Strenght in Glasses, Glass Science and Technology, Vol. 5. Academic Press, New York, NY, pp. 133–145.

Freiman, S.W., 1980. Fracture mechanics of glass. In: Elasticity and Strenght in Glasses, Glass Science and Technology, Vol. 5. Academic Press, New York, NY, pp. 21–78.

Halbach, H. and Chatterjee, N.D., 1982. An empirical Redlich–Kwong-type equation of state of water to 1,000°C and 200 kbar. Contrib. Mineral. Petrol., 79: 337–345.

Hardee, H.C., 1980. Solidificatiion in Kilauea Iki lava lake. J. Volcanol. Geotherm. Res., 7: 211–233.

Holtz, F., Behrens, H., Dingwell, D.B. and Johannes, W., 1995. H_2O solubility in haplogranitic melts: Compositional, pressure, and temperature dependence. Am. Mineral., 80: 94–108.

Hurwitz, S. and Navon, O., 1994. Bubble nucleation in rhyolitic melts: experiments at high pressure, temperature and water content. Earth Planet. Sci. Lett., 122: 267–280.

Inglis, C.E., 1913. Stresses in a plate due to the presence of cracks and sharp corners. R. Inst. Naval Arch. Trans., 55: 219–230.

Jaupart, C. and Allègre, C.J., 1991. Gas content, eruption rate and instabilities of eruption regime in silicic volcanoes. Earth Planet. Sci. Lett., 102: 4513–429.

Karsten, J.L., Holloway, J.R. and Delaney, J.R., 1982. Ion microprobe studies of water in silicate melts: temperature-dependent water diffussion in obsidian. Earth Planet. Sci. Lett., 59: 420–428.

Kress, V.C. and Carmichael, I.S.E., 1991. The compressibility of silicate liquids containing Fe_2O_3 and the effect of composition, temperature, oxygen fugacity and pressure on their redox states. Contrib. Mineral. Petrol., 108: 82–92.

Kress, V.C., Williams, Q. and Carmichael, I.S.E., 1989. When is a silicate melt not liquid? Geochim. Cosmochim. Acta, 53: 1687–1692.

Lange, R.A., 1994. The effect of H_2O, CO_2 and F on the density and viscosity of silicate melts. In: Volatiles in Magmas. Rev. Mineral., 30: 331–369.

Lapham, K.E., Holloway, J.R. and Delaney, J.R., 1984. Diffusion of H_2O and D_2O in obisidian at elevated temperatures and pressures. J. Non-Cryst. Solids, 67: 179–191.

Lawn, B.R., 1993. Fracture of Brittle Solids. Cambridge Univ. Press, Cambridge, 2nd ed, 378 pp.

MacMillan, P.F., 1994. Water solubility and speciation models. In: Volatiles im Magmas. Rev. Mineral., 30: 131–156.

Manghnani, M.H., Sato, H. and Rai, C.S., 1986. Ultrasonic velocity and attenuation measurements on basalt melts to 1500°C: role of composition and structure in the viscoelastic properties. J. Geophys. Res., 91: 9333–9342.

Mazurin, O.V., Streltsina, M.V. and Shvaiko-Shvaikovskaya, T.P., 1983. Handbook of Glass Data. Part A. Silica Glass and Binary Silicate Glasses. Elsevier, Amsterdam.

Melson, W.G., 1983. Monitoring the 1980–1982 eruptions of Mount St. Helens: compositions and abundances of glass. Science, 221: 1387–1391.

Mungall, J.E., 1994. Interfacial tension in miscible two-fluid systems with linear viscoelastic rheology. Phys. Rev. Lett., 73: 288–291.

Mungall, J.E., 1995. Textural controls on explosivity of lava in Merapi-type block and ash flows. Per. Mineral., 64: 233–234.

Newman, S., Stolper, E.M. and Epstein, S., 1986. Measurement of water in rhyolitic glasses: calibration of an infrared spectroscopic technique. Am. Mineral., 71: 1527–1541.

Newman, S., Epstein, S. and Stolper, E.M., 1988. Water, carbon dioxide, and hydrogen isotopes in glasses from the ca. 1340 eruption of the Mono Craters, California: constraints on degassing phenomena and initial volatile content. J. Volcanol. Geotherm. Res., 35: 75–96.

Nowacki, W., 1986. Thermoelasticity. Pergamon, Frankfurt, 2nd ed.

Nowak, M. and Behrens, H., 1995. The speciation of water in haplogranitic glasses and melts determined by in situ near-infrared spectroscopy. Geochim. Cosmochim. Acta, 59: 3445–3450.

Paillat, O., Elphick, S.C. and Brown, W.L., 1992. The solubility of water in $NaAlSi_3O_8$ melts: a re-examination of Ab–H_2O phase relationships and critical behavior at high pressures. Contrib. Mineral. Petrol., 112: 490–500.

Pineau, F. and Javoy, M., 1994. Strong degrassing at ridge crests: the behavior of dissolved carbon and water in basalt glasses at 14°N, Mid-Atlantic Ridge. Earth Planet. Sci. Lett., 123: 179–198.

Pollard, D.D., 1987. Elementary fracture mechanics applied to the structural interpretation of dykes. In: H.C. Halls and W.F. Fahrig (Editors), Mafic Dyke Swarms. Geol. Assoc. Can., Spec. Pap., 34: 5–24.

Roedder, E., 1984. Fluid inclusions. Rev. Mineral. 12, 644 pp.

Romano, C., Dingwell, D.B., Bagdassarov, N. and Mungall, J.E., 1994a. The tensile strength of vesicular magma: experimental constraints from the stability of synthetic fluid inclusions in melts. Eos, 75: 725.

Romano, C., Dingwell, D.B. and Sterner, S.M., 1994b. Kinetics of quenching of hydrous feldspathic melts: qualification using synthetic fluids inclusions. Am. Mineral., 79: 1125–1134.

Romano, C., Dingwell, D.B. and Behrens, H., 1995. The temperature dependence of the speciation of water in $NaAlSi_3O_8$–$KAlSi_3O_8$ melts: and application of fictive temperatures derived from synthetic fluid-inclusions. Contrib. Mineral. Petrol., 122: 1–10.

Romano, C., Mungall, J.E., Dingwell D.B., Bagassarov, N. and Sharp, T., 1996. Tensile strengths of vesicular glasses: An experimental study. Am. Mineral., in press.

Sato, H., Fujii, T. and Nakada, S., 1992. Crumbling of dacite dome lava and generation of pyroclastic flows at Unzen volcano. Nature, 360: 664–666.

Self, S., Wilson, L. and Nairn, I.A., 1979. Vulcanian eruption mechanisms. Nature, 227: 440–443.

Shaw, H.R., 1974. Diffusion of H_2O in granitic liquids. Part I, experimental data, Part II, mass transfer in magma chambers. In: A.W. Hoffman, B.J. Gilletti, H.S. Yoder and R.A. Yund (Editors), Geochemical Transport and Kinetics. Carnegie Inst. Washington, DC, pp. 201–264.

Shen, A. and Keppler, H., 1995. Infrared spectroscopy of hydrous silicate melts to 1000°C and 10 kbars: direct observation of water speciation in a diamond anvil cell. Am. Mineral., 80: 1335–1338.

Silver, L.A., Ihinger, P.D. and Stolper, E., 1990. The influence of bulk composition on the speciation of water in silicate glasses. Contrib. Mineral. Petrol., 104: 142–162.

Snyder, D., Gier, E. and Carmichael, I., 1994. Experimental measurements of the thermal conductivity of molten silicates. Mineral. Mag., 858–859.

Spera, F.J., 1980. Aspects of magma transport. In: R.B. Hargraves (Editor), Physics of Magmatic Processes. Princeton Univ. Press, Princeton, NJ, pp. 265–324.

Stevenson, R.J., Dingwell, D.B., Webb, S.L. and Bagdassarov, N.S., 1995. The equivalence of enthalpy and shear stress relaxation in rhyolitic obsidians and quantification of the liquid–glass transition in volcanic processes. J. Volcanol. Geotherm. Res., 68: 297–306.

Stolper, E., 1982. The speciation of water in silicate melts. Geochim. Cosmochim. Acta, 46: 2609–2620.

Taylor, B.E., Eichelberger, J.C. and Westrich, H.R., 1983. Hydrogen isotopic evidence of rhyolitic magma degassing during intrusion and eruption. Nature, 306: 541–545.

Tsuchida, E., Saito, Y., Nakahara, I. and Kodama, M., 1982.

Stresses in a semi-infinite body containing a prolate spheroidal cavity subjected to an axisymmetric pressure. Bull. Jpn. Soc. Miner. Eng., 25: 891–897.

Wasserburg, G.J., 1988. Diffusion of water in silicate melts. J. Geol., 96: 363–367.

Webb, S.L., 1991. Shear and volume relaxation in $Na_2Si_2O_5$. Am. Mineral., 76: 1449–1454.

Webb, S.L. and Dingwell, D.B., 1990. The onset of non-newtonian rheology of silicate melts a fibre elongation study. Phys. Chem. Miner., 17: 125–132.

Wilson, L. and Head III, J.W., 1981. Ascent and eruption of basaltic magma on the Earth and Moon. J. Geophys. Res., 86: 2971–3001.

Woods, A.W. and Koyaguchi, T., 1994. Transitions between explosive and effusive eruptions of silicic magmas. Nature, 370: 641–644.

Zhang, Y., Stolper, E.M. and Wasserburg, G.J., 1991. Diffusion of water in rhyolitic glasses. Geochim. Cosmochim. Acta, 55: 441–456.

Zhang, Y., Stolper, E.M. and Ihinger, P.D., 1995. Kinetics of the reaction $H_2O + O = 2OH$ in rhyolitic and albitic glasses: preliminary results. Am. Mineral., 80: 593–612.